Transcriptional responses of the *Trichoplusia ni* midgut to oral infection by the baculovirus Autographa californica Multiple Nucleopolyhedrovirus

Anita Shrestha[1*], Kan Bao[1], Wenbo Chen[1], Ping Wang[2], Zhangjun Fei[1], and Gary W. Blissard[1#]

[1]Boyce Thompson Institute at Cornell University, Tower Road, Ithaca NY 14853

[2]Department of Entomology, Cornell University, Geneva, NY 14456

Running Head: Midgut transcriptional responses to AcMNPV

#Address correspondence to:
Gary W. Blissard, Boyce Thompson Institute at Cornell University
533 Tower Road, Ithaca, NY 14853 Phone: 607-254-1366
Email: gwb1@cornell.edu

*Present address: Exonics Therapeutics, Inc., Boston, MA

Abstract word count: 224
Text word count: 8284

Running Title: *Trichoplusia ni* midgut responses to AcMNPV infection

Keywords: *Trichoplusia ni*, midgut, transcriptome, Baculovirus, AcMNPV, differential expression, immune genes

ABSTRACT

Baculoviruses are large dsDNA viruses that are virulent pathogens of certain insect species. In a natural host, *Trichoplusia ni,* infection by the model baculovirus Autographa californica Multiple Nucleopolyhedrovirus (AcMNPV) begins when the occluded form of the virus disassembles in the midgut and virions infect midgut epithelial cells to establish the primary phase of the infection. To better understand the primary phase of the AcMNPV infection cycle, newly molted 5th instar *T. ni* larvae were orally infected with AcMNPV occlusion bodies and transcriptional responses of the *T. ni* midgut were analyzed at various times from 0-72 hours post infection, using RNA-Seq analysis and a *T. ni* reference genome. The numbers of differentially expressed host genes increased as the infection progressed, and we identified a total of 3,372 differentially expressed *T. ni* transcripts in the AcMNPV-infected midgut. Genes encoding orthologs of HMG176, atlastin, and CPH43 were among the most dramatically upregulated in response to AcMNPV infection. A number of cytochrome P450 genes were downregulated in response to infection. We also identified the effects of AcMNPV infection on a large variety of genes associated with innate immunity. This analysis provides an abundance of new and detailed information on host responses to baculovirus infection during the primary phase of the infection in the midgut, and will be important for understanding how baculoviruses establish productive infections in the organism.

IMPORTANCE

Baculoviruses are virulent pathogens of a number of important insect pest species. In the host *Trichoplusia ni*, infection begins in the midgut when infectious virions of the occulsion derived virus (ODV) phenotype enter and subsequently replicate in cells of the midgut epithelium. A second virion phenotype (budded virus or BV) is produced there and BV mediates systemic infection of the animal. Most prior detailed studies of baculovirus infections have focused on BV infections of cultured cells. In this study, we examined the transcriptional responses of the *T. ni* midgut to infection by ODV of the baculovirus AcMNPV, and identified a variety of host genes that respond dramatically to viral infection. Understanding transcriptional responses of the host midgut to viral

infection is critically important for understanding the biphasic infection in the animal as a whole.

INTRODUCTION

Baculoviruses are arthropod-specific viruses with circular dsDNA genomes ranging from approximately 80 to 180 kbp that are packaged in rod-shaped nucleocapsids (1-3). Baculoviruses are used as biological control agents for agriculturally important insect pests in the order Lepidoptera (4). In general, baculovirus species have very narrow host ranges, often limited to one or a few closely related insect species (5). *Autographa californica Multiple Nucleopolyhedrovirus* (AcMNPV) is the type species of the family *Baculoviridae* and is the most intensively studied model of baculovirus biology. Unlike many other baculoviruses, AcMNPV has a wide host range, infecting at least 33 species of lepidopteran larvae in 10 families (1, 6). AcMNPV is highly pathogenic in early instar larvae of some species, yet less pathogenic in other species and when infecting later instars (7, 8).

Baculoviruses such as AcMNPV that have been studied extensively, produce two virion phenotypes: the Occlusion Derived Virus (ODV) and the Budded Virus (BV). ODV and BV are physically and functionally distinct, with BV produced initially by nucleocapsid budding from the surface of infected cells, and ODV produced later by nucleocapsid envelopment within the nucleus. ODV, which is subsequently occluded in a crystallized protein occlusion body (OB), is released into the environment and is orally infectious. When consumed by a susceptible host, OBs disassemble in the larval midgut, releasing ODV that subsequently enter midgut epithelial cells and initiate the primary phase of the infection in the animal. During the primary phase of the infection in the midgut, BV bud from the basal surfaces of midgut cells and BV subsequently infect most other tissues, initiating the secondary phase of the infection (reviewed in references (2) and (1)). The majority of detailed studies of baculovirus infection and host responses have focused on infections of cultured cells by BV (representing the secondary phase of infection), yet the primary phase of the infection is critically important to the success of infection in the organism. In a prior study of AcMNPV infection of *Heliothis virescens*

and *Helicoverpa zea* (representing permissive and semi-permissive hosts), it was observed that even though susceptibility to mortal infection differed by >1000-fold, detection of viral infection in the midgut appeared to be similar (9). Thus, the differences in host susceptibility appear to occur at a stage following viral entry into midgut cells, and responses of the midgut cells to infection may be critical for success of the primary infection and subsequent systemic infection. Differences in midgut intracellular responses to viral infection may lead to differences in production of infectious progeny virions, or differences in signaling or immune activation at the organismal level. Although midgut responses to AcMNPV infection are clearly important, and likely determine the outcome of infection in the host, little detail is known about midgut responses, even in highly permissive host insects such as *Trichoplusia ni* (the cabbage looper). To understand how midgut cells react to AcMNPV infection, we used a high throughput sequencing approach to measure the effects of oral infection by AcMNPV ODV on global host gene expression in the *Trichoplusia ni* larval midgut. We previously performed a similar study of global host gene expression using a *T. ni* cell line (Tnms42) that was synchronously infected with AcMNPV BV (10, 11). BV infection of cultured Tnms42 cells is thought to most closely represent a model of events in the secondary phase of infection in the animal. Initiation of ODV infection of the midgut epithelium is substantially less efficient than synchronous infection of cultured cells by BV in the laboratory. High doses of ODV result in infection of only a subset of midgut epithelial cells in 5th instar larvae. However, midgut cells that are infected by ODV may receive a relatively high dose of the virus since ODV virions contain multiple nucleocapsids. Because the midgut represents a first line of defense in oral infection by invading pathogens, the responses of midgut cells in the primary phase of infection may differ substantially from responses of cultured cells to BV infection, which represent the secondary phase of infection.

Prior studies have shown that baculovirus infection triggers antiviral and other immune responses in cultured cells (1, 12, 13). In this study, we compared transcriptomes of control (uninfected) and AcMNPV-infected *T. ni* midgut tissue, and identified *T. ni* transcripts that were either up- or downregulated at each time point (0, 6, 12, 18, 24, 36, 48, and 72 h p.i.) following oral infection by ODV. Differential expression analysis resulted in the identification of a total of 3,372 transcripts with at least 4-fold changes

(FC) in expression levels. Functional annotations of these differentially expressed (DE) transcripts revealed overall trends in important host cellular processes affected by virus infection. Of particular interest, AcMNPV infection dramatically increased expression levels of several genes (HMG176, atlastin-2, cuticle CPH43, and E3 ubiquitin-ligase SIAH) in infected midgut, whereas expression levels of several other genes (flippase, serine protease 33, and a variety of cytochrome P450 genes) were dramatically reduced. We also identified a small subset of *T. ni* transcripts that were differentially expressed across all time points postinfection. Thus, the global transcriptional analysis of AcMNPV-infected *T. ni* midgut provides a detailed characterization of midgut-specific cellular responses to baculovirus infection and will be important for understanding the complex virus-host interactions in the primary phase of infection.

MATERIALS AND METHODS

Insects and viruses

Methods for insect rearing, AcMNPV infection, generation of viruses and preparation of RNA-Seq libraries were described in detail previously (14) and are briefly summarized below. *T.ni* (Cornell Strain) eggs were obtained from the Wang laboratory at Cornell University (Geneva, NY). Eggs on wax paper sheets (app. 4 days old) were surface sterilized by immersion in 10% Clorox, rinsed with sterile deionized water, and air-dried. Eggs were then placed in 16 oz. cups containing artificial-wheat germ diet and maintained in a growth chamber at 27 °C with a Light:Dark photoperiod of 14:10 as described previously (14). Fourth instar larvae that were ready to molt were held for 0-5 h without diet and newly molted 5^{th} instar larvae (0-5 h old) were used for oral infections.

Wild Type AcMNPV strain E2 (WT-AcMNPV) used for the study was purified, amplified, and titered (15) as described previously (14). *T. ni* cell line Tnms42 (an alphanodavirus-free cell line subcloned from High Five, BTI-Tn5B14 cells) (11, 16, 17) was then infected with BV of WT-AcMNPV at a MOI of 0.1 and maintained in TNM-FH medium (18) (Invitrogen) supplemented with 2.5% FBS at 28°C. After 7 days, OBs were collected and purified using 0.5% SDS and 0.5 M NaCl as previously described (15), and resuspended in 10 ml of H_2O. Similar to WT-AcMNPV, OBs from a recombinant baculovirus carrying a 2^{nd} copy of the viral capsid protein (VP39) that was fused to 3

copies of the mCherry marker gene (virus 3mC) (19) were prepared and fed to larvae to determine the minimum number of OBs required to obtain maximum midgut cell infection in *T. ni* larvae. We estimated that the maximal infection rate was approximately 20-30% of the midgut cells by 48 h p.i.

Larvae were orally inoculated with occlusion bodies (OBs) of WT-AcMNPV by hand feeding 5th instar larvae with 5 µl of a 10% sucrose solution containing a total of 7×10^4 OBs of WT-AcMNPV (1.4×10^4 OBs/µl). Mock-infected control larvae were fed a similar sucrose solution containing no virus. At one-hour post feeding, control or virus-inoculated larvae (about 30 each) were placed in a growth chamber at 27 ºC as described above. Midgut tissue was dissected at eight time points postinfection: 0, 6, 12, 18, 24, 36, 48, 72 hours post infection (h p.i.). Thus, for each time point sampled post infection, a parallel mock-infected control midgut sample was analyzed, to mitigate possible artifacts resulting from developmental changes that may occur over the course of the experiment. For each time point and treatment (infected or control), we prepared three replicate samples, with midgut samples from six larvae pooled for each replicate. For each dissection, the larval cuticle was cut longitudinally along the dorsal midline and pinned in a dissecting dish, then the midgut was cut anteriorly and posteriorly and removed with forceps, avoiding excessive tracheoles. The excised midgut (which is approximately 70-80% of the length of the 5th instar larva) contained the midgut epithelium, plus the closely attached layer of muscle and some attached tracheoles. Excised midgut samples did not contain malpighian tubules, fatbody, or excessive tracheoles or hemocytes. The excised gut was washed by dipping in chilled PBS (two or more times), then immediately placed in RNA*later*® RNA stabilization solution (Ambion) on ice. Pooled midgut samples were stored at -70°C, then homogenized with a pestle in a 1.5 ml eppendorf tube, and total RNA extraction was performed with TRIzol reagent (Ambion) according to the manufacturers protocol. Following total RNA extraction, midgut RNAs were screened by PCR for a known *T. ni* tetravirus (data not shown), and only tetravirus negative midguts were used for experiments.

RNA-Seq library preparation

Strand-specific RNA-Seq libraries were constructed as described previously (14, 20). Briefly, poly(A) mRNAs isolated from 3 µg of total RNA using oligo(dT)25

Dynabeads (Invitrogen) were fragmented at 94°C for 5 min in buffer containing ProtoScript II reaction buffer (NEB), hexamer (Qiagen), and oligo $(dT)_{23}$ VN (NEB). Subsequently, first-strand cDNA was synthesized using ProtoScript II and second strand synthesis was carried out with a reaction mix consisting of RNase H (NEB), the Klenow fragment of DNA polymerase I (NEB), and a dNTP mix containing dATP, dCTP, dGTP, and dUTP (Promega Corporation). Next, TruSeq universal adapters were ligated to the end-repaired and dA-tailed cDNA fragments. The dUTP containing strands were then removed and PCR amplification was performed with library-specific TruSeq PCR primers. Following purification and quantification, libraries were sequenced on the Illumina HiSeq4000 platform at the CLC Genomics and Epigenomics Core Facility at the Weill Cornell Medical College.

RNA-Seq read processing and differential expression analysis

Raw RNA-Seq reads were processed using Trimmomatic software (21) with default parameters to trim adapter and low quality sequences, and trimmed reads with length <40 bases were discarded. Ribosomal RNA reads were removed by aligning the reads to rRNA sequences using bowtie (22). Filtered reads were then mapped to the *T.ni* reference genome (23) using HISAT (24) allowing 2 mismatches. Based on the alignments, raw read counts of each *T. ni* gene were derived and normalized to Reads Per Kilobase of transcript per Million mapped reads (RPKM) (25). Subsequently, differentially expressed (DE) transcripts between the uninfected and infected midgut samples at different time points postinfection were identified using edgeR package (26). Transcripts with a FDR (false discovery rate) lower than 0.05 and a ≥4-fold change in expression levels were classified as DE transcripts.

Functional annotation, Venn diagrams, and cluster analysis

Annotations of differentially expressed transcripts following virus infection were identified by searching for homologous sequences against the NCBI non-redundant (nr) protein database using BLASTP with an *E*-value cutoff of 10^{-5}. To further obtain gene ontology (GO) terms associated with DE transcripts, we used Blast2GO software (https://www.blast2go.com) (27). Using the GO database, GO terms were assigned to the DE transcripts under biological process with an *E*-value hit filter of 10^{-6} and an annotation cutoff of 55. The GO terms were classified at GO level 4. We constructed

Venn diagrams to identify DE transcripts that are commonly expressed between different time points postinfection and also across time points postinfection. For Venn diagram construction, we classified time points into three major groups: Early (0, 6, 12, 18 h p.i.), Middle (24, 36 h p.i.) and Late (48 and 72 h p.i.). For each group, we combined induced and upregulated transcripts from each time point. Similarly, we also combined suppressed and downregulated transcripts from each time point. We also performed cluster analysis on normalized expression levels (log2(RPKM)) of DE transcripts across time points by applying Euclidean distance metric using DESeq2 software (28). From the list of genes grouped by cluster analysis, we identified *T. ni* transcripts with specific expression patterns such as genes with expression levels that increased or decreased consistently over the infection time points.

Identification of most significantly affected *T. ni* transcripts and expression patterns of immune genes in the midgut

From the list of differentially expressed transcripts identified in this study, we further identified *T. ni* transcripts with the most significant changes by setting a threshold of a 16-fold change (16-FC) in expression levels. We included only transcripts with RPKM values of $\geq$ 50 for infected (for upregulated or induced) or uninfected (for downregulated or suppressed) midgut samples. Further, in the previous study, homologs of several immune response specific genes (from yeasts, human, *Drosophila melanogaster*, *Bombyx mori*, *S. exigua*, or *S. frugiperda*) were identified in Tnms42 cells (10). In the current study, we identified homologs of immune gene transcripts (previously identified in Tnms42 cells) in the *T. ni* insect reference genome (23) using BLAST and analyzed expression patterns of the immune genes in the *T. ni* midgut across time points postinfection.

RESULTS AND DISCUSSION

Differential expression analysis of *T. ni* transcripts following AcMNPV infection

To analyze midgut cell responses to AcMNPV infection, developmentally synchronized and newly molted 5th instar *T. ni* larvae were orally infected with WT-AcMNPV OBs as described previously (14). Each larva was orally inoculated with 7×10^4

OBs, a dose determined empirically as the minimum approximate dose resulting in maximal numbers of infected midgut cells. At selected time points postinfection (0, 6, 12, 18, 24, 36, 48, and 72 h p.i.) midguts were excised and pooled (6 larval midguts per replicate; 3 replicates per time point) and used for isolation of polyA mRNA and construction of strand-specific RNA-Seq libraries for Illumina sequencing. From each replicate sample, we mapped cleaned reads to the *T. ni* reference genome (14,384 genes) (23). Previously, we also estimated viral reads in each *T. ni* midgut sample by similarly mapping cleaned reads to the AcMNPV genome (156 genes) (NCBI accession no. NC_001623) (14). The percentage of total reads mapping to *T. ni* genes declined gradually as the infection proceeded (Fig. 1 and Table 1), with the largest decline in *T. ni* read counts observed between 36 and 72 h p.i., when the percentage of viral reads simultaneously increased most dramatically (Fig. 1). To identify changes in *T. ni* transcript levels that resulted from AcMNPV infection, we estimated expression levels of each *T. ni* gene by calculating RPKM levels (Table S1), and performed differential expression analysis between AcMNPV-infected and uninfected midgut at each of the selected time points postinfection. We only considered transcripts with at least a 4-fold change (4-FC) in transcript levels (between the infected and uninfected samples) as differentially expressed (DE) transcripts. Using this threshold, we identified a total of 3,372 DE *T. ni* transcripts in the AcMNPV-infected midgut (Fig. 2, and Table S2A-B). At early time points (0, 6, 12 h p.i.) few DE transcripts were detected (67 DE transcripts total), while substantial numbers of DE transcripts were identified at later times: 18 h p.i. (424 transcripts), 24 h p.i. (82 transcripts), 36 h p.i. (414 transcripts), 48 h p.i. (475 transcripts), and 72 h p.i. (1910 transcripts) (Table S2A-B). In general and as expected, DE transcript numbers increased as the infection proceeded. We further sub-classified DE transcripts (4-FC and $p<0.05$) based on the degree of up- or downregulation at each time point. For these calculations, RPKM values of <1 were treated as 0. Therefore, *T. ni* transcripts with RPKM values of <1 in one of the midgut samples (uninfected or infected) were classified as either induced or suppressed, respectively, in response to AcMNPV infection (Table S2-A). For example, a transcript with an RPKM value of <1 in the uninfected midgut and ≥ 1 in the infected midgut at a time point was classified as induced, while a transcript with an RPKM value of ≥ 1 in the uninfected midgut and <1

in the infected midgut was classified as suppressed. If transcript RPKM values were ≥ 1 in both infected and uninfected midguts (and they differed by ≥4-fold), they were classified as either upregulated or downregulated (Table S2-B). Using these criteria, we identified a total of 920 (induced), 1419 (upregulated), 578 (suppressed), and 455 (downregulated) transcripts in the midgut (Fig. 2).

Functional annotation of differentially expressed *T. ni* transcripts

To identify possible functions of the DE transcripts affected by the virus infection in the *T. ni* midgut, we searched for homologs of the *T. ni* transcripts in the non-redundant database at NCBI using BLASTP. We identified potential orthologs for 60% of the induced transcripts, 93% of the upregulated transcripts, 70% of the suppressed transcripts, and 83% of the downregulated transcripts (Table S2A-B, Annotation). Blast2GO analysis was also performed on DE transcripts to identify major biological processes that were affected by the virus infection. For a broad overview, we combined DE transcripts from all time points for each classified DE group (induced, upregulated, suppressed, and downregulated) and performed Blast2GO analysis on each DE group. Blast2GO assigned 25 and 26 GO terms to upregulated and induced transcripts, respectively (Fig. 3A and C), and 11 and 16 GO terms to downregulated and suppressed transcripts, respectively (Fig. 3B and D). Among the GO terms assigned to upregulated transcripts, many of the transcripts were associated with cellular protein modification (11%), response to stress (7 %), DNA metabolic process (7%), ribosome biosynthesis (7%), chromosome organization (6%), signal transduction (5%), and cell differentiation (4%). Further, GO terms of induced transcripts (under the biological process) were primarily associated with metabolic processes such as macromolecule metabolic process (10%), cellular nitrogen compound metabolic process (10%), organic cyclic compound metabolic process (8%), and heterocycle metabolic process (7.8%). For transcripts that were downregulated in the AcMNPV infected midgut, GO terms included nitrogen compound metabolic process (14%), biosynthetic process (12%), single-organism cellular process (10%), and response to stimulus (7%). Analysis of suppressed transcripts resulted in GO terms involved in transport (10%), oxidation and reduction (6%), protein metabolism (6%), and cellular macromolecule metabolic process (5%).

T. ni transcripts differentially expressed between and across time points postinfection

Next we examined transcripts that were differentially expressed during several time periods postinfection (Fig. 4). We first divided time periods into three categories: Early (12 and 18 h p.i.), Middle (24 and 36 h p.i.) and Late (48 and 72 h p.i.). The earliest times sampled in our experiments (0 and 6 h p.i.) were not included as we identified very few DE transcripts at those times (Tables S2A and S2B). We examined induced + upregulated transcripts from each time point for one set of comparisons (Fig. 4A), and suppressed + downregulated transcripts for another set of comparisons (Fig. 4B). Venn diagrams illustrate the numbers of common DE transcripts within each category: Early, Middle, or Late. For the induced + upregulated DE transcripts, we identified 56, 39, and 272 shared DE transcripts within the Early, Middle, and Late categories, respectively (Fig. 4A, Table S3). No suppressed + downregulated DE transcripts were identified as shared between 12 and 18 h p.i., but 18 and 83 DE transcripts in that category were shared within the Middle and Late periods, respectively (Fig. 4B, Table S3). We also identified transcripts that were differentially expressed across most time points (from 12 to 72 h p.i.) and they are listed in Table 2. Of these, we identified 11 transcripts that were induced or upregulated across all times sampled from 12-72 h postinfection. These transcripts included HMG176 (a REsponse to Pathogen or REPAT gene), atlastin-2, E3 ubiquitin-ligase SIAH1, cyclic GMP-AMP synthase isoform X2, mitochondrial uncoupling 4, and NF-kappa-B-repressing factor. In the case of suppressed or downregulated transcripts, 14 transcripts were differentially expressed across time points from 18-72 h p.i. (Table 2). Examples of these transcripts include serine protease 33, folylpolyglutamate synthase, Ves G 1 allergen, indole-3-glycerol phosphate synthase, flippase, and DNA mismatch repair protein (Table 2, Suppressed and Downregulated). Levels of several of these up- or downregulated transcripts (such as HMG176, atlastin-2, flippase, and serine protease 33) were radically different in infected midgut cells, with differences of up to 640-fold. Several of these genes are discussed in more detail in the section below (see also Table 3).

Cluster analysis of differentially expressed *T. ni* transcripts

We also grouped differentially expressed *T. ni* transcripts identified in this study using hierarchical cluster analysis. We selected transcripts that were differentially expressed (between uninfected and infected midguts) by ≥ 4-fold and performed cluster analysis on the expression levels, then we identified patterns of expression of those transcripts from the infected midgut. A heatmap generated from the cluster analysis (Figure 5A) shows the DE transcripts grouped into five clusters. We arbitrarily referred to the groups as G1, G2, G3, G4, and G5 (Fig 5A), which are comprised of 34, 201, 697, 1,433, and 205 transcripts, respectively, and these transcripts are listed in Table S4. From the list of DE transcripts grouped by cluster analysis, we performed a separate analysis to identify transcripts with specific expression patterns (Fig. 5B). We identified transcripts with four expression patterns: P1, continuously increasing; P2, continuously decreasing; P3, increasing from 0-18 h p.i. then decreasing; and P4, reaching the highest levels at 12-18 h p.i. (Fig. 5B). Specific *T. ni* transcripts within each of these groups from Figure 5B are listed in Table S5. We identified nine transcripts that continuously increased from 0 to 72 h p.i. (Fig. 5B, P1), and 17 transcripts with levels that decreased continuously from 0 to 72 h p.i. (Fig. 5B, P2). Examples of transcripts from pattern P1 included: mismatch repair endonuclease, intracellular transport US1, N-acetyltransferase, and ribonuclease H1. Among transcripts from pattern P2 were: larval cuticle 8 protein, a cuticular RR-2 family protein, regucalcin isoform, and sodium potassium transporting ATPase subunit-2. Further we identified 22 transcripts conforming to pattern P3 (including insect intestinal lipase, glucose dehydrogenase, prophenoloxidase subunit 1, peroxisome membrane PMP34, and laminin subunit alpha isoform X3). We found that 96 transcripts were associated with pattern P4, with examples including genes encoding HMG176 isoform (REPAT proteins), atlastin-2 like isoform 1, cecropin B, prophenoloxidase 2, lipase 3, cytochrome P450, ecdysone oxidase, aldehyde oxidase, serine proteases 31, and an ankyrin repeat domain protein (Table S5).

T.ni genes most significantly affected by AcMNPV infection

A. Induced and upregulated T. ni transcripts

From a comprehensive list of differentially expressed *T. ni* transcripts (Table S2A and Table S2B), we identified the most significantly affected of the differentially

366 expressed transcripts, based on the RPKM values (minimum value of 50 RPKM for either
367 uninfected or infected cells), or a change of at least 16-fold between uninfected and
368 infected midgut cells. We subdivided the DE transcript groups into the following
369 categories: induced, upregulated, suppressed, and downregulated. Using these thresholds
370 and groupings, we identified 63 transcripts with large differences in transcript levels
371 (Table 3). Below, we highlight several of the DE genes that were of particular interest.

372 **i. HMG176 (REPAT)**

373 *T. ni* orthologs of a gene named *HMG176* (29) were significantly upregulated or
374 induced and highly expressed in response to AcMNPV infection in the midgut. *T. ni*
375 orthologs of HMG176 were either substantially induced or upregulated in the midgut
376 from 12 to 72 h p.i. (Tables 3 and S7). HMG176 belongs to a gene family encoding small
377 proteins (11-17 kDa) called REPAT (REsponse to Pathogens) proteins, that were initially
378 identified from *Spodoptera exigua* larval midgut challenged with either *Bacillus*
379 *thuringiensis* toxin Cry1Ca or with baculovirus AcMNPV. REPAT proteins were later
380 identified in other lepidopteran species (30-34) (See also "REPAT genes" below). The
381 *HMG176* gene of *Helicoverpa armigera* is normally expressed at high levels in midguts
382 of molting larvae and the protein is found in the basal lamina of the midgut of molting
383 and feeding larvae, but not in larvae committed to metamorphosis (29, 35). The precise
384 function of HMG176 is not known. In contrast to the relatively early induction of
385 HMG176 observed in the AcMNPV-infected *T. ni* larval midgut, some REPAT genes
386 appear to be induced much later after AcMNPV infection of *S. exigua* larvae, with
387 induction of some detected after approximately 72 h p.i. (30). Because the *H. armigera*
388 HMG176 gene is upregulated during molting in uninfected larvae (29), it is possible that
389 its dramatic upregulation in response to AcMNPV infection of the midgut may represent
390 the activation of some genes associated with the molting process, perhaps as a defensive
391 response by the host, or as a viral-induced mechanism to facilitate dissemination of the
392 virus in the infected host.

393 **ii. Atlastin**

394 Another highly upregulated *T. ni* transcript is an atlastin-2 ortholog
395 (Tni05G05890). The *T. ni* atlastin-2 ortholog was dramatically upregulated in the midgut
396 following oral infection with AcMNPV. Transcript levels were increased (9-111 fold) at

various times from 12-72 h p.i., and the highest degree of upregulation occurred at early times in the infection: 12 h p.i. (81 fold) and 18 h p.i. (111 fold) (Tables 3 and S2B). Atlastin proteins are close homologs to guanylate-binding proteins (GBPs), and are in the dynamin superfamily of proteins (36). The GBPs include MX proteins, which are well-studied interferon-induced antiviral proteins in vertebrates (37). Functionally, atlastins are involved in endoplasmic reticulum (ER) network formation and fusion, and vesicle trafficking in the ER (38, 39). Recently, a member of the atlastin protein family (atlastin-n) was shown to provide resistance to baculovirus infection in *Bombyx mori* (40). When the atlastin-n protein was overexpressed in *B. mori* BmN-SWU1 cells or in larvae, virus production was inhibited, suggesting an antiviral role against BmNPV. The dramatic upregulation of the atlastin-2 ortholog in AcMNPV-infected *T. ni* midgut may represent an induced antiviral response to AcMNPV infection, although more direct studies will be required to understand its role following oral infection.

iii. CPH43

We also identified a *T. ni* ortholog (Tni08G03170) of the hypothetical cuticle protein CPH43 gene of *B. mori*, as one of the most significantly upregulated transcripts in the infected *T. ni* midgut. The extensively studied *B. mori* genome contains approximately 255 cuticular protein genes, of which 44 were identified as hypothetical cuticular protein (CPH) genes based on indirect evidence (41). In the current study, CPH43 transcript levels were upregulated in the AcMNPV-infected *T. ni* midgut by approximately 18-157 fold (18-72 h p.i.) with extremely high transcript levels at 72 h p.i. (Table 3). Similar to the current study, transcript levels of CPH43 were also shown to increase in *B. mori* midgut tissues following pathogenic infection with *Bombyx mori* cytoplasmic polyhedrosis virus (BmCPV), and CPH43 upregulation was speculated to play a role in remodeling of the midgut epithelium (42).

iii. cGAS orthologs

We observed upregulation of transcripts of several *T. ni* isoforms of cyclic guanosine monophosphate - adenosine monophosphate synthase (cyclic GMP-AMP synthase or cGAS) genes (Tni22G05470, Tni22G05480, and Tni22G05460), in the infected *T. ni* midgut. Among the three substantially upregulated *T. ni* cGAS transcripts, the most highly expressed and most dramatically upregulated was Tni22G05470, which

was upregulated by as much as 59- and 47-fold (12 and 18 h p.i.) and was present at high RPKM levels (approximately 150 and 82) at relatively early times post infection (12 and 18 h p.i.) (Tables 3 and S2B). The other two *T. ni* cGAS transcripts were also upregulated at earlier times, but were most dramatically upregulated [by as much as 10-fold (Tni22G05460) and 33-fold (Tni22G05480)] at later times post infection (72 h p.i.). cGAS is a cytosolic DNA sensor that binds to foreign DNA such as viral pathogens and induces activation of the type I interferon pathway and NF-kB signaling, to defend against infections by viruses such as retroviruses and herpesviruses (43, 44). While insects do not have an interferon response pathway, NF-kB signaling is known to activate innate immune responses. The upregulation of cGAS transcripts in the midgut at early time points in the infection suggests that AcMNPV infection may result in a systemic activation of immune responses throughout the midgut tissue. Future studies to examine the specific mechanistic role(s) of cGAS in infected and bystander cells could yield important details on how cells and the midgut tissue overall react to viral infection in the midgut.

iv. Mucin-5AC-like gene

Further, among the dramatically induced or upregulated transcripts was a mucin-like gene, identified as the *mucin-5AC-like* gene. We observed upregulation of mucin-5AC-like transcripts (Tni03G01880) at most times postinfection in the midgut (Table 3) with upregulation ranging from approximately 6.5-58 fold at times from 18-72 h p.i. and very high RPKM values ranging from approximately 310 to 1524. The localization and function of the mucin-5AC-like protein are unknown. Previously an insect intestinal mucin (IIM) (Tni02G02610) was identified as a major component of the peritrophic membrane (PM), the semipermeable structure that lines the midgut and serves as a structural barrier to viral infection (45-47). The IIM transcripts were present at extremely high levels (RPKM of 1050-7430) and were modestly upregulated (1.4-3.6 fold) over the 72 h of infection of the midgut. In some (probably most) baculovirus infections, viral-encoded proteases (such as the enhancin protein) target IIM for degradation, resulting in loss of PM integrity and thereby enhancing virus infection (47). The upregulation of mucin transcript levels observed in the *T. ni* midgut as a response to infection (Table 3) may represent a general response to PM disruption, and a defense mechanism against

459 virus-mediated PM degradation. In a prior study of the midgut of another noctuid species
460 (*Spodoptera frugiperda*) it was found that degradation of the PM by a maize cysteine
461 protease resulted in upregulation and increased abundance of IIM mRNAs (48, 49).
462 Other transcripts of note that were highly upregulated in the midgut in response to
463 oral AcMNPV infection were orthologs of an E3 ubiquitin ligase SIAH (Tni17G02340),
464 a Zinc finger CCHC (Tni12G01690), a peroxidase (isoform X2, Tni22G00330), and a
465 chymotrypsin-like serine protease (Tni18G02870) (Table 3).
466 ***B. Suppressed and downregulated transcripts***
467 We also identified a significant number of *T. ni* transcripts that were either
468 suppressed or downregulated (at least 16-fold) in the midgut in response to AcMNPV
469 infection. Some of the most strikingly suppressed or downregulated transcripts included
470 orthologs of flippase, serine proteases, cytochrome P450, calcium binding protein P, and
471 dehydroecdysone 3 alpha-reductase (Table 3).
472 **i. Flippase**
473 Flippases are transmembrane proteins that mediate lipid transport between leaflets
474 of a lipid bilayer and they may be associated with formation of vesicles (50, 51). We
475 found that flippase transcripts, which are highly abundant in uninfected control midgut
476 tissue (RPKM values were as high as 2246), were dramatically downregulated from at
477 least 18 h p.i.. How reduced flippase might affect the infection or the defense of the host
478 is unclear.
479 **ii. Serine Protease 33**
480 The transcript levels of a chymotrypsin-like serine protease (Serine protease 33,
481 Tni18G00450) were also significantly suppressed by AcMNPV infection (Table 3, and
482 S2A). Serine proteases play diverse roles in physiological processes, notably digestion in
483 the midgut, apoptosis, development, and immunity (52, 53).
484 **iii. Cytochrome P450**
485 Cytochrome P450 proteins are enzymes that are involved in biosynthesis and
486 metabolism (including detoxification) of a large variety of molecules. They are encoded
487 by a large gene family and the number of cytochrome P450 genes varies widely among
488 lepidopteran species: ranging from approximately 78 to over 100 (54). While the P450
489 genes of *T. ni* have not been studied in detail, the automated annotation of the *T. ni*

genome (23) identified approximately 118 genes as potential P450 genes. (Note: Some of these may represent fragments or pseudogenes as a recent study identified at least 18 pseudogenes in another lepidopteran genome (54).) While some *T. ni* cytochrome P450 orthologs were upregulated in response to AcMNPV infection, we observed suppression or downregulation of a substantial number of cytochrome P450 orthologs (Tni16G04090, Tni16G04370, Tni16G04420, Tni16G04430, Tni15G02520, Tni22G05060, Tni09G03330, Tni10G04110, Tni15G06560, Tni15G06570, Tni15G06610, Tni21G02490, Tni21G02470, Tni21G02450, Tni21G03890, Tni21G03910, Tni17G05560, Tni21G02490, Tni21G01940, Tni17G05570) in the midgut, following AcMNPV infection (Tables S2A and S2B). The downregulation of P450 genes following baculovirus infection was also observed in *H. zea* (55), suggesting that baculovirus-mediated suppression of P450s could play an important role in suppressing metabolic pathways in the insect host during the infection process.

iv. Other genes

Following virus infection, transcripts encoding several digestive enzymes, including lipase 3 and carboxypeptidase M, were significantly lower in infected midgut samples (Table 3). Digestive enzymes have been shown to have antiviral activities against viral pathogens. In contrast to observations here, baculovirus-infected *B. mori*, midgut-specific digestive enzymes including lipase-1 and serine proteases-2 were induced by virus infection, and these enzymes were speculated to inactivate ODV in the midgut (56, 57). We also observed significant downregulation of transcripts potentially involved in regulation of the ecdysone signaling pathway, including 3-dehydroecdysone 3alpha-reductase and ecdysone oxidase (Table 3).

C. Antiviral, immune, and stress response genes

After identifying DE transcripts that were most significantly affected by virus infection in the *T. ni* midgut, we analyzed expression patterns of transcripts associated with stress response and immune pathways in the *T. ni* midgut. Orthologs of a variety of immune response genes from yeasts, human, *Drosophila melanogaster*, *B. mori*, *S. exigua*, or *S. frugiperda* were identified in a prior study of a *T. ni* (Tnms42 cell line) transcriptome (10), and the corresponding genes and transcripts were identified in the recently assembled *T. ni* genome (23), and used for analysis in this study. Expression

patterns of immune response and stress response-related genes were compared in uninfected and infected *T. ni* midgut (Fig. S1, A-L) and RPKM values and fold changes are shown in Table S6. Transcripts with RPKM values less than 5 across all times postinfection in both uninfected and infected midguts were not included in this analysis.

i. Small interfering RNAs

RNA interference (RNAi) is an antiviral response in invertebrates that detects double-stranded RNAs. dsRNA is diced into small interfering RNAs (siRNAs) which interact with an RNAase III enzyme and the resulting RNA-induced silencing complex (RISC) directs the cleavage of complementary RNAs in a sequence-specific manner. In insects, RNAi is a major antiviral defense mechanism against invading RNA and DNA viruses (58, 59). In a prior study of AcMNPV infected Tnms42 cells, downregulation of RNAi pathway associated genes such as Argonaute-2 (Ago-2) and Dicer-2 (Dcr-2) was described (10). In the current study of responses to oral AcMNPV infection in the *T. ni* midgut, we found that transcript abundance of Ago-2, Dcr-2, R3D1, and R2D2 increased slightly (by >2-fold) in the infected midgut by 12 h p.i., and substantially (>5-fold) by 72 h p.i.. (Fig. S1A, and Table S6). For Dcr-2 and R2D2, expression levels in the infected midgut were even higher, >13-fold and >12-fold, respectively (Fig. S1,A and Table S6). Dcr-2 is an RNase III enzyme that interacts with R2D2 and binds to and cleaves dsRNA into siRNAs. The siRNAs are loaded into the Ago-2 containing RISC which then cleaves the targeted RNA (58). The observed upregulation of major components of RNAi pathways including Dcr-2, R2D2, and Ago-2 in the AcMNPV infected midgut (beginning around 12-18 h p.i.), indicates that AcMNPV infection induces components of the RNAi response in the *T. ni* midgut.

ii. REPAT genes

REPAT (REsponse to PAThogens) genes were initially identified as genes that were upregulated in the *Spodoptera exigua* midgut, in response to bacterial (*B. thuringiensis*) or viral (AcMNPV) challenge, and REPAT genes have been identified in other insect species (30-34). REPAT genes represent a large gene family in *S. exigua* (46 REPAT genes identified) (33) and closely related species also have numerous REPAT genes (35 in *S. frugiperda*; 21 in *S. litura*; 13 in *S. littoralis*; and 8 in *M. configurata*). Of the 8 REPAT genes in *M. configurata*, 6 are isoforms of HMG176, which we identified

as one of the most highly upregulated genes in the AcMNPV-infected *T. ni* midgut (see above). For some other insect species (*M. brassicae*, *B. mori*, *H. armigera*, and *D. melanogaster*), only a single REPAT gene has been identified (33, 34). Thus far, the precise biochemical or molecular roles of REPAT proteins have not been identified, although they appear to play a variety of roles. While HMG176 is found in the basal lamina of the midgut (29, 35), another REPAT protein (MBF2 from *B. mori*) was identified as a transcriptional co-activator (33, 60). The single identified *Drosophila* REPAT gene (*CG13323*) was reported to be upregulated in response to infection with bacteria, fungi, and sigma virus (61), but the function of the encoded protein is unknown. The wide diversity in sequence and expression profiles among REPAT proteins suggest that they may serve a variety of functions, perhaps as a group of stress-response proteins with antiviral or antimicrobial functions. Interestingly, while overexpression of the *S. exigua* REPAT 1 protein from a recombinant baculovirus had no apparent effect on virus amplification in cultured Sf21 cells, injections of BV from the REPAT 1-expressing baculovirus into *S. exigua* larvae resulted in delayed mortality when compared with a control virus (30), suggesting a possible antiviral role.

A blast search of the *T. ni* genome (23) revealed at least 12 REPAT genes (Table S7). Three of the *T. ni* REPAT genes (Tni20G02130, Tni20G02140, and Tni20G02110) encode isoforms of HMG176 and were highly induced or upregulated upon oral infection with AcMNPV (Tables 3, S2A, and S2B). One of the HMG176 transcripts (Tni20G02130) was induced dramatically in the midgut at 12-48 h p.i. (with an RPKM value of >90 at 12 h p.i.) and upregulated by approximately 80 fold at 72 h p.i. (Tables 3, S2A, and S2B). Based on sequence similarities of the 12 identified REPAT genes in the *T. ni* genome (by comparison with REPAT genes from multiple insect orders (33)), we assigned the *T. ni* REPAT genes to phylogenetic groupings identified among the REPAT genes. Of the 12 *T. ni* REPAT genes, 6 are assigned to Group III, 2 to Group V, and 1 each to Groups I, IV, and VI. One gene (Tni28G00730) was closely similar to a REPAT gene (REPAT27) that was not assigned to one of the 6 phylogenetic groupings (Table S7).

iii. Melanization

Melanization is a component of the insect innate immune response that is involved in encapsulation of invading pathogens and parasites, and also associated with wound repair. Key components in the process of melanization are serine proteases (SPs) that regulate cleavage of prophenoloxidase (proPO) through a serine protease cascade, to generate active phenoloxidase (53, 62) Phenoloxidase mediates the production of melanin, which traps or encapsulates pathogens and parasites, and may close wounds. Serine protease inhibitors regulate the activity of this cascade. We noted reduced levels of two transcripts encoding prophenoloxidase components by 72 h p.i. (Tni16G00190 and Tni16G03510) and one serine protease inhibitor (Tni25G00940); but substantial increases were observed in the transcript levels of three serine protease inhibitors (Tni15G03410, Tni03G03940, and Tni22G04260) (Fig. S1B and Table S6, Melanization). Overall, these varied changes in transcript levels suggest that baculovirus AcMNPV infection may modulate melanization in the *T. ni* midgut. Downregulation of melanization was previously observed in *S. exigua* larvae (63) and *H. armigera* following baculovirus infection (64).

iii. Apoptosis

As an immune response, apoptosis or programmed cell death can prevent systemic viral infection by detecting and eliminating infected cells. The triggering and regulation of apoptosis is tightly controlled by a cascade of initiator and effector proteases known as caspases. While baculovirus infections can induce apoptosis in insect cells, baculoviruses are able to block the anti-viral apoptotic response of the host (65-67). Baculoviruses encode protein inhibitors of apoptosis such as P35 and IAP (Inhibitor of Apoptosis), which may inhibit the initiation or execution of the apoptotic cascade (67-70). We examined the effects of WT AcMNPV infection on the midgut expression patterns of apoptosis-related host genes including caspase genes, cytochrome-c, p53, reaper, and others (Fig. S1C-D and Table S6). We annotated caspase genes according to the orthologs identified in *B. mori*, *D. melanogaster*, *S. exigua*, and *S. frugiperda,* similar to an earlier study of Tnms42 cells (10). Notable among the apoptosis-associated genes, the transcript levels of 8 genes were substantially upregulated (>4 fold). These upregulated genes include Fas-associated protein with death domain (FADD,

612 Tni22G02980), caspase-4 (Tni20G00950), caspase-6-Dredd (Tni10G01580), apoptosis
613 inducing factor (*aif*) (Tni14G00370), p53 (Tni16G04470), caspase-1 (Tni23G04710), and
614 Htra2 (Tni19G03780 and Tni19G03770) (Table S6). In comparison to these observations
615 in the *T. ni* midgut, AcMNPV infection in the Tnms42 cell line resulted in decreased
616 caspase transcript levels in Tnms42 cells (10). It is unclear why midgut cells respond
617 differently than cultured Tnms42 cells in this regard, but such differences could reflect
618 functional specialization of the midgut cells as a first barrier to infection in the animal.
619 **iv. Heat shock proteins**
620 Heat shock proteins (HSPs) are stress-response proteins that are induced
621 following biotic and abiotic stress (71). In Drosophila, loss of heat shock transcription
622 factor reduced resistance to infection by several viruses, suggesting the importance of
623 heat shock proteins in anti-viral defense (72). To examine the effects of AcMNPV
624 infection on HSPs, we analyzed expression patterns of HSPs in the *T. ni* midgut after
625 challenge with AcMNPV OBs. Transcript levels of approximately 30% of the HSPs
626 examined increased by >4 fold in AcMNPV-infected midguts, compared with uninfected
627 midguts (Table S6 and Fig. S1E-F). However, transcript levels of seven HSP genes were
628 dramatically (>8 fold) increased at certain times post infection, and these genes included
629 heat shock binding protein 70 (Tni29G01390), hsp19.5 (Tni05G00200), hsp20.8
630 (Tni27G00120), hsp70 (Tni08G01440), small heat shock protein 19.7 (Tni27G00160),
631 and small heat shock proteins (Tni05G06500, Tni27G00130, and Tni05G06520) (Table
632 S6). In prior studies of AcMNPV-infected Sf9 cells, an increase in hsp70 levels was
633 observed following infection, and inhibition of the heat shock response resulted in
634 decreased viral DNA replication and reduced production of infectious BV (73). In
635 addition, hsp70 was dramatically upregulated in the midgut of *Helicoverpa zea* larvae
636 that were orally infected with Helicoverpa zea single nucleopolyhedrovirus (HzSNPV)
637 (74). Interestingly, HSP70 was found in gradient purified virions of both BV and ODV of
638 BmNPV, and in both envelope and capsid fractions of BV (75). Thus, while the precise
639 role(s) of hsp70 in baculovirus infections is not clear, prior studies have established the
640 importance of hsp70 during various steps of infection by other viruses (76, 77) and, also
641 in association with antiviral responses (78). In addition to hsp70, the other heat shock

642 proteins that were substantially upregulated in response to midgut infection may also play
643 important roles in antiviral and/or antimicrobial defenses in the midgut.
644 **v. Reactive oxygen species (ROS)**
645 ROS are chemically reactive molecules containing oxygen, that are normal
646 metabolic products that may be increased during cellular stress, such as infections by
647 pathogens. ROS directly kill pathogens in the phagolysosomes of innate immune cells
648 and also initiate innate immune signaling (79). Baculovirus infection induces oxidative
649 stress in infected cells (80). For most ROS related genes examined in this study, we did
650 not observe substantial differences in transcript levels between the infected and
651 uninfected midguts (Table S6 and Fig. S1, G). However, genes such as catalase,
652 superoxide dismutase (SOD), and cytochrome P450 showed moderate increases in
653 transcript levels at several times from 18-48 h p.i. (Fig. S1, G).
654 **vi. Innate immune pathways**
655 To avoid infection by invading bacteria and fungi, insect defenses typically involve
656 innate immunity pathways that include Toll, JAK/STAT, JNK, and IMD. Components of
657 these pathways have also been implicated in antiviral responses but their roles in antiviral
658 defenses remain unclear and poorly defined (81-83). Immune genes associated with these
659 pathways are typically involved in pathogen recognition, signaling, and production of
660 antimicrobial peptides that degrade and disrupt pathogens. To examine the effects of
661 AcMNPV infection on midgut expression of these pathways, we selected representative
662 genes associated with NF-kB-IkB, JAK/STAT, JNK, IMD, and Toll signaling pathways,
663 similar to an earlier study (10), and analyzed the expression patterns of each gene in the
664 uninfected and AcMNPV-infected *T. ni* midgut. In general, expression of genes
665 associated with NFkB-IkB pathway increased following virus infection (Table S6;
666 NFkB-IKB), with transcripts of 4 of the 5 genes examined increasing by approximately
667 3-6 fold by 72 h p.i. (Fig. S1,H; Table S6; Tni12G04870, Tni09G01890, Tni12G00240,
668 Tni19G05340). Among the members of JAK/STAT pathway (Fig. S1,I), transcript levels
669 of some genes were modestly upregulated after 12-18 h p.i., while others did not appear
670 to change substantially. The more dramatically upregulated of these JAK/STAT pathway
671 genes were Domeless (Tni09G04150), MEKK1 (Tni06G03240), P38B (Tni03G00270),
672 and STAT92E (Tni29G00500), which were upregulated by 4-15 fold in the infected

673 midgut compared to uninfected midgut. Of the 9 JNK pathway associated genes
674 examined, most transcript levels were moderately upregulated (2-4 fold) as infection
675 progressed in the midgut (Fig. S1,J; Table S6, JNK). Among the 38 IMD and Toll
676 pathway genes examined, transcript levels remained mostly unchanged or were
677 moderately increased (Table S6, IMD and Toll). However AcMNPV infection in the
678 midgut resulted in more dramatic increases for approximately 10 IMD and Toll pathway
679 genes at various times post infection. These more dramatically upregulated genes were
680 upregulated by approximately 4-13 fold and included Toll 7 (Tni23G01350), CG13422
681 (Tni07G01830), dorsal isoforms (Tni09G01890 and Tni12G00240), GNBP3 isoforms
682 (Tni11G00720 and Tni11G00760), PGRPESA (Tni09G00600 and Tni16G02760),
683 SERPINE27A (Tni07G01400), and TRAF2 (Tni13G00780) (Table S6, IMD and Toll;
684 Fig. S1, K and L). The moderate upregulation of these genes in the infected midgut may
685 represent a more generalized response to infection in the midgut, but could also represent
686 direct antiviral responses. Additional and more specific studies that specifically target
687 these genes and their gene products will be required to better understand innate immune
688 responses to baculovirus infection in the midgut.

689 **SUMMARY**

690 Our recent studies of AcMNPV transcription in the midgut and cell line (11, 14)
691 revealed substantial differences in transcription of certain viral genes, and suggest a
692 midgut-specific program of viral gene expression. The primary stage of baculovirus
693 infection in the lepidopteran midgut is critical for success of the virus and the responses
694 by the cells of the midgut include important host defensive reactions to infection. The
695 transcriptional responses by the host midgut must certainly encompass a variety of
696 strategies to prevent productive viral replication in the midgut and transmission of the
697 infection to other tissues of the insect host. Because the primary stage of infection by
698 baculoviruses typically involves direct infection and replication in only a subset of the
699 cells of the midgut as a whole, the results reported in this study represent responses by
700 both the directly infected cells, and uninfected bystander cells of the midgut. Thus many
701 of the responses observed here may represent responses to signaling from infected cells,
702 as well as to viral disruption of the normal midgut physiological status. It is also likely
703 that the virus may direct signaling that enhances viral replication and transmission of the

704 virus from the midgut into the tissues of the hemocoel. The biology of the midgut and
705 midgut infection are enormously complex, and it is critically important to understand
706 how the midgut globally responds to viral infection, as well as how viruses potentially
707 manipulate the midgut and enhance their transmission. The global expression data
708 provided here represent an early step toward understanding these complex interactions.
709 As the transcriptome provides only a snapshot of the effects of viral infection on host
710 transcript levels, future studies will need to examine a variety of additional factors,
711 including topics such as virus-induced changes in translation efficiency, post-translational
712 modifications, and protein turnover. Combined, these and other studies should aid in the
713 utilization of beneficial viruses such as baculoviruses in applications in biological control
714 of important pest insects. In addition, a more detailed understanding of virus-cell
715 interactions in the midgut may also be useful for developing new strategies for inhibiting
716 the insect transmission of problematic viruses.
717
718

719 **ACKNOWLEDGEMENTS**

720 We thank Yimin Xu for generous help with RNA-Seq libraries, Jenny Xiang for
721 help with Illumina sequencing, and Wendy Kain for *T. ni* eggs and larvae. This work was
722 supported by grants from the USDA (2015-67013-23281) to GWB, PW, and ZF, and
723 from the NSF (IOS-1354421, 1653021) to GWB. RNA-Seq data were submitted to the
724 NCBI SRA under Bioproject No. PRJNA484772.
725

REFERENCES

1. **Rohrmann GF.** 2013. Baculovirus Molecular Biology: Third Edition., *on* National Center for Biotechnology Information (US). http://www.ncbi.nlm.nih.gov/pubmed/24479205. Accessed 2018.
2. **Blissard GW, Theilmann DA.** 2018. Baculovirus Entry and Egress from Insect Cells. Annu Rev Virol **5:**113-139.
3. **Herniou EA, Arif BM, Becnel JJ, Blissard GW, Bonning B, Harrison R, Jehle JA, Theilmann DA, Vlak JM.** 2011. *Baculoviridae*, p 163-173. *In* King AMQ, Adams MJ, Carstens EB, Lefkowitz EJ (ed), Virus Taxonomy: Ninth Report of the International Committee on Taxonomy of Viruses. Elsevier Academic Press, New York.
4. **Popham HJ, Nusawardani T, Bonning BC.** 2016. Introduction to the Use of Baculoviruses as Biological Insecticides. Methods Mol Biol **1350:**383-392.
5. **Federici BA.** 1997. Baculovirus pathogenesis, p 39-59. *In* Miller LK (ed), The Baculoviruses. Plenum Press, New York.
6. **Groner A.** 1986. Specificity and safety of baculoviruses, The Biology of Baculoviruses. CRC Press, Boca Raton, Florida.
7. **Haas-Stapleton EJ, Washburn JO, Volkman LE.** 2003. Pathogenesis of Autographa californica M nucleopolyhedrovirus in fifth instar *Spodoptera frugiperda*. J Gen Virol **84:**2033-2040.
8. **Kirkpatrick BA, Washburn JO, Volkman LE.** 1998. AcMNPV pathogenesis and developmental resistance in fifth instar *Heliothis virescens*. J Invertebr Pathol **72:**63-72.
9. **Trudeau D, Washburn JO, Volkman LE.** 2001. Central role of hemocytes in *Autographa californica* M nucleopolyhedrovirus pathogenesis in *Heliothis virescens* and *Helicoverpa zea*. J Virol **75:**996-1003.
10. **Chen YR, Zhong S, Fei Z, Gao S, Zhang S, Li Z, Wang P, Blissard GW.** 2014. Transcriptome responses of the host, *Trichoplusia ni*, to infection by the baculovirus, *Autographa californica* Multiple Nucleopolyhedrovirus (AcMNPV). J Virol **88:**13781-13797.
11. **Chen YR, Zhong S, Fei Z, Hashimoto Y, Xiang JZ, Zhang S, Blissard GW.** 2013. The transcriptome of the baculovirus *Autographa californica* Multiple Nucleopolyhedrovirus (AcMNPV) in *Trichoplusia ni* cells. J Virol **87:**6391-6405.
12. **Clem RJ.** 2005. The role of apoptosis in defense against baculovirus infection in insects. Curr Top Microbiol Immunol **289:**113-129.
13. **Jayachandran B, Hussain M, Asgari S.** 2012. RNA interference as a cellular defense mechanism against the DNA virus, baculovirus. J Virol **86:**13729-13734.
14. **Shrestha A, Bao K, Chen YR, Chen W, Wang P, Fei Z, Blissard GW.** 2018. Global analysis of baculovirus Autographa californica Multiple Nucleopolyhedrovirus gene expression in the midgut of the lepidopteran host *Trichoplusia ni*. J Virol **92:**e01277-01218.
15. **O'Reilly DR, Miller LK, Luckow VA.** 1992. Baculovirus expression vectors, a laboratory manual. W. H. Freeman and Co., New York.
16. **Granados RR, Li GX, Derksen ACG, Mckenna KA.** 1994. A new insect cell line from *Trichoplusia ni* (BTI-Tn-5B1-4) susceptible to *Trichoplusia ni* single enveloped nuclear polyhedrosis virus. J Invertebr Pathol **64:**260-266.

17. **Koczka K, Peters P, Ernst W, Himmelbauer H, Nika L, Grabherr R.** 2018. Comparative transcriptome analysis of a *Trichoplusia ni* cell line reveals distinct host responses to intracellular and secreted protein products expressed by recombinant baculoviruses. J Biotechnol **270:**61-69.
18. **Hink WF.** 1970. Established insect cell line from the cabbage looper, *Trichoplusia ni*. Nature **226:**466-467.
19. **Ohkawa T, Volkman LE, Welch MD.** 2010. Actin-based motility drives baculovirus transit to the nucleus and cell surface. J Cell Biol **190:**187-195.
20. **Zhong S, Joung JG, Zheng Y, Chen YR, Liu B, Shao Y, Xiang JZ, Fei Z, Giovannoni JJ.** 2011. High-throughput Illumina strand-specific RNA sequencing library preparation. Cold Spring Harb Protoc **2011:**940-949.
21. **Bolger AM, Lohse M, Usadel B.** 2014. Trimmomatic: a flexible trimmer for Illumina sequence data. Bioinformatics **30:**2114-2120.
22. **Langmead B.** 2010. Aligning short sequencing reads with Bowtie. Curr Protocols in Bioinformatics **Chapter 11:**Unit 11 17.
23. **Chen W, Yang X, Tetreau G, Song X, Coutu C, Hegedus D, Blissard G, Fei Z, Wang P.** 2018. A high-quality chromosome-level genome assembly of a generalist herbivore, *Trichoplusia ni*. Mol Ecol Resour doi:10.1111/1755-0998.12966**:***Published OnLine: 18 November 2018*.
24. **Kim D, Langmead B, Salzberg SL.** 2015. HISAT: a fast spliced aligner with low memory requirements. Nat Methods **12:**357-360.
25. **Mortazavi A, Williams BA, McCue K, Schaeffer L, Wold B.** 2008. Mapping and quantifying mammalian transcriptomes by RNA-Seq. Nat Methods **5:**621-628.
26. **Robinson MD, McCarthy DJ, Smyth GK.** 2010. edgeR: a Bioconductor package for differential expression analysis of digital gene expression data. Bioinformatics **26:**139-140.
27. **Conesa A, Gotz S, Garcia-Gomez JM, Terol J, Talon M, Robles M.** 2005. Blast2GO: a universal tool for annotation, visualization and analysis in functional genomics research. Bioinformatics **21:**3674-3676.
28. **Love MI, Huber W, Anders S.** 2014. Moderated estimation of fold change and dispersion for RNA-seq data with DESeq2. Genome Biol **15:**550.
29. **Wang JL, Jiang XJ, Wang Q, Hou LJ, Xu DW, Wang JX, Zhao XF.** 2007. Identification and expression profile of a putative basement membrane protein gene in the midgut of *Helicoverpa armigera*. BMC Dev Biol **7:**76.
30. **Herrero S, Ansems M, Van Oers MM, Vlak JM, Bakker PL, de Maagd RA.** 2007. REPAT, a new family of proteins induced by bacterial toxins and baculovirus infection in *Spodoptera exigua*. Insect Biochem Mol Biol **37:**1109-1118.
31. **Hernandez-Marinez P, Navarro-Cerrillo G, Caccia S, de Maagd RA, Moar WJ, Ferre J, Escriche B, Herrero S.** 2010. Constitutive activation of the midgut response to *Bacillus thuringiensis* in Bt-Resistant *Spodoptera exigua*. PLoS ONE **5:**e12795.
32. **Navarro-Cerrillo G, Ferre J, de Maagd RA, Herrero S.** 2012. Functional interactions between members of the REPAT family of insect pathogen-induced proteins. Insect Mol Biol **21:**335-342.

33. **Navarro-Cerrillo G, Hernandez-Martinez P, Vogel H, Ferre J, Herrero S.** 2013. A new gene superfamily of pathogen-response (repat) genes in Lepidoptera: classification and expression analysis. Comp Biochem Physiol B Biochem Mol Biol **164:**10-17.
34. **Machado V, Serrano J, Galian J.** 2016. Identification and characterization of pathogen-response genes (repat) in *Spodoptera frugiperda* (Lepidoptera: Noctuidae). Folia Biol (Krakow) **64:**23-29.
35. **Dong DJ, He HJ, Chai LQ, Jiang XJ, Wang JX, Zhao XF.** 2007. Identification of genes differentially expressed during larval molting and metamorphosis of *Helicoverpa armigera*. BMC Dev Biol **7:**73.
36. **Praefcke GJK.** 2017. Regulation of innate immune functions by guanylate-binding proteins. Int J Med Microbiol doi:10.1016/j.ijmm.2017.10.013.
37. **Verhelst J, Hulpiau P, Saelens X.** 2013. Mx proteins: antiviral gatekeepers that restrain the uninvited. Microbiol Mol Biol Rev **77:**551-566.
38. **Namekawa M, Muriel MP, Janer A, Latouche M, Dauphin A, Debeir T, Martin E, Duyckaerts C, Prigent A, Depienne C, Sittler A, Brice A, Ruberg M.** 2007. Mutations in the SPG3A gene encoding the GTPase atlastin interfere with vesicle trafficking in the ER/Golgi interface and Golgi morphogenesis. Mol Cell Neurosci **35:**1-13.
39. **Hu J, Shibata Y, Zhu PP, Voss C, Rismanchi N, Prinz WA, Rapoport TA, Blackstone C.** 2009. A class of dynamin-like GTPases involved in the generation of the tubular ER network. Cell **138:**549-561.
40. **Liu TH, Dong XL, Pan CX, Du GY, Wu YF, Yang JG, Chen P, Lu C, Pan MH.** 2016. A newly discovered member of the Atlastin family, BmAtlastin-n, has an antiviral effect against BmNPV in Bombyx mori. Sci Rep **6:**28946.
41. **Liang J, Zhang L, Xiang Z, He N.** 2010. Expression profile of cuticular genes of silkworm, *Bombyx mori*. BMC Genomics **11:**173.
42. **Kolliopoulou A, Van Nieuwerburgh F, Stravopodis DJ, Deforce D, Swevers L, Smagghe G.** 2015. Transcriptome analysis of *Bombyx mori* larval midgut during persistent and pathogenic cytoplasmic polyhedrosis virus infection. PLoS One **10:**e0121447.
43. **Li XD, Wu J, Gao D, Wang H, Sun L, Chen ZJ.** 2013. Pivotal roles of cGAS-cGAMP signaling in antiviral defense and immune adjuvant effects. Science **341:**1390-1394.
44. **Gao D, Wu J, Wu YT, Du F, Aroh C, Yan N, Sun L, Chen ZJ.** 2013. Cyclic GMP-AMP synthase is an innate immune sensor of HIV and other retroviruses. Science **341:**903-906.
45. **Terra WR.** 2001. The origin and functions of the insect peritrophic membrane and peritrophic gel. Arch Insect Biochem Physiol **47:**47-61.
46. **Lehane MJ.** 1997. Peritrophic matrix structure and function. Annu Rev Entomol **42:**525-550.
47. **Wang P, Granados RR.** 1997. An intestinal mucin is the target substrate for a baculovirus enhancin. Proc Natl Acad Sci U S A **94:**6977-6982.
48. **Pechan T, Ye L, Chang Y, Mitra A, Lin L, Davis FM, Williams WP, Luthe DS.** 2000. A unique 33-kD cysteine proteinase accumulates in response to larval

feeding in maize genotypes resistant to fall armyworm and other Lepidoptera. Plant Cell **12:**1031-1040.

49. **Fescemyer HW, Sandoya GV, Gill TA, Ozkan S, Marden JH, Luthe DS.** 2013. Maize toxin degrades peritrophic matrix proteins and stimulates compensatory transcriptome responses in fall armyworm midgut. Insect Biochem Mol Biol **43:**280-291.

50. **Devaux PF, Herrmann A, Ohlwein N, Kozlov MM.** 2008. How lipid flippases can modulate membrane structure. Biochim Biophys Acta **1778:**1591-1600.

51. **Daleke DL.** 2003. Regulation of transbilayer plasma membrane phospholipid asymmetry. J Lipid Res **44:**233-242.

52. **Srinivasan A, Giri AP, Gupta VS.** 2006. Structural and functional diversities in lepidopteran serine proteases. Cell Mol Biol Lett **11:**132-154.

53. **Cao X, He Y, Hu Y, Zhang X, Wang Y, Zou Z, Chen Y, Blissard GW, Kanost MR, Jiang H.** 2015. Sequence conservation, phylogenetic relationships, and expression profiles of nondigestive serine proteases and serine protease homologs in *Manduca sexta*. Insect Biochem Mol Biol **62:**51-63.

54. **Calla B, Noble K, Johnson RM, Walden KKO, Schuler MA, Robertson HM, Berenbaum MR.** 2017. Cytochrome P450 diversification and hostplant utilization patterns in specialist and generalist moths: Birth, death and adaptation. Mol Ecol **26:**6021-6035.

55. **Noland JE, Breitenbach JE, Popham HJ, Hum-Musser SM, Vogel H, Musser RO.** 2013. Gut transcription in *Helicoverpa zea* is dynamically altered in response to baculovirus infection. Insects **4:**506-520.

56. **Ponnuvel KM, Nakazawa H, Furukawa S, Asaoka A, Ishibashi J, Tanaka H, Yamakawa M.** 2003. A lipase isolated from the silkworm *Bombyx mori* shows antiviral activity against nucleopolyhedrovirus. J Virol **77:**10725-10729.

57. **Nakazawa H, Tsuneishi E, Ponnuvel KM, Furukawa S, Asaoka A, Tanaka H, Ishibashi J, Yamakawa M.** 2004. Antiviral activity of a serine protease from the digestive juice of *Bombyx mori* larvae against nucleopolyhedrovirus. Virology **321:**154-162.

58. **Gammon DB, Mello CC.** 2015. RNA interference-mediated antiviral defense in insects. Curr Opin Insect Sci **8:**111-120.

59. **Bronkhorst AW, van Cleef KWR, Vodovar N, İnce İA, Blanc H, Vlak JM, Saleh M-C, van Rij RP.** 2012. The DNA virus Invertebrate Iridescent Virus 6 is a target of the *Drosophila* RNAi machinery. Proc Natl Acad Sci U S A **109:**E3604-E3613.

60. **Liu QX, Ueda H, Hirose S.** 2000. MBF2 is a tissue- and stage-specific coactivator that Is regulated at the step of nuclear transport in the silkworm *Bombyx mori*. Dev Biol **225:**437-446.

61. **Carpenter J, Hutter S, Baines JF, Roller J, Saminadin-Peter SS, Parsch J, Jiggins FM.** 2009. The transcriptional response of *Drosophila melanogaster* to infection with the sigma virus (Rhabdoviridae). PLoS One **4:**e6838.

62. **Kanost MR, Gorman MG.** 2008. Phenoloxidases in insect immunity, p 69-96. *In* Beckage N (ed), Insect Immunology. Academic Press/Elsevier, San Diego.

63. **Jakubowska AK, Vogel H, Herrero S.** 2013. Increase in gut microbiota after immune suppression in baculovirus-infected larvae. PLoS Pathog **9:**e1003379.

64. **Yuan C, Xing L, Wang M, Wang X, Yin M, Wang Q, Hu Z, Zou Z.** 2017. Inhibition of melanization by serpin-5 and serpin-9 promotes baculovirus infection in cotton bollworm *Helicoverpa armigera*. PLoS Pathog **13:**e1006645.
65. **Clem RJ, Fechheimer M, Miller LK.** 1991. Prevention of apoptosis by a baculovirus gene during infection of insect cells. Science **254:**1388-1390.
66. **Lerch RA, Friesen PD.** 1993. The 35-kilodalton protein gene p35 of Autographa californica nuclear polyhedrosis virus and the neomycin resistance gene provide dominant selection of recombinant baculoviruses. Nucleic Acids Res **21:**1753-1760.
67. **Clem RJ, Popham HJR, Shelby KS.** 2010. Antiviral responses in insects: apoptosis and humoral responses, p 453. *In* Asgari S, Johnson KN (ed), Insect Virology. Caister Academic Press.
68. **Clem RJ.** 2007. Baculoviruses and apoptosis: a diversity of genes and responses. Curr Drug Targets **8:**1069-1074.
69. **Byers NM, Vandergaast RL, Friesen PD.** 2016. Baculovirus Inhibitor-of-Apoptosis Op-IAP3 blocks apoptosis by interaction with and stabilization of a host insect cellular IAP. J Virol **90:**533-544.
70. **Means JC, Clem RJ.** 2008. Evolution and function of the p35 family of apoptosis inhibitors. Future Virology **3:**383-391.
71. **King AM, MacRae TH.** 2015. Insect heat shock proteins during stress and diapause. Annu Rev Entomol **60:**59-75.
72. **Merkling SH, Overheul GJ, van Mierlo JT, Arends D, Gilissen C, van Rij RP.** 2015. The heat shock response restricts virus infection in *Drosophila*. Sci Rep **5:**12758.
73. **Lyupina YV, Dmitrieva SB, Timokhova AV, Beljelarskaya SN, Zatsepina OG, Evgen'ev MB, Mikhailov VS.** 2010. An important role of the heat shock response in infected cells for replication of baculoviruses. Virology **406:**336-341.
74. **Breitenbach JE, Popham HJ.** 2013. Baculovirus replication induces the expression of heat shock proteins in vivo and in vitro. Arch Virol doi:10.1007/s00705-013-1640-8.
75. **Iwanaga M, Shibano Y, Ohsawa T, Fujita T, Katsuma S, Kawasaki H.** 2014. Involvement of HSC70-4 and other inducible HSPs in Bombyx mori nucleopolyhedrovirus infection. Virus Res **179:**113-118.
76. **Baquero-Perez B, Whitehouse A.** 2015. Hsp70 isoforms are essential for the formation of Kaposi's sarcoma-associated herpesvirus replication and transcription compartments. PLoS Pathog **11:**e1005274.
77. **Taguwa S, Maringer K, Li X, Bernal-Rubio D, Rauch JN, Gestwicki JE, Andino R, Fernandez-Sesma A, Frydman J.** 2015. Defining Hsp70 subnetworks in dengue virus replication reveals key vulnerability in flavivirus infection. Cell **163:**1108-1123.
78. **Kim MY, Ma Y, Zhang Y, Li J, Shu Y, Oglesbee M.** 2013. hsp70-dependent antiviral immunity against cytopathic neuronal infection by vesicular stomatitis virus. J Virol **87:**10668-10678.
79. **Schieber M, Chandel NS.** 2014. ROS function in redox signaling and oxidative stress. Curr Biol **24:**R453-462.

80. **Wang Y, Oberley LW, Murhammer DW.** 2001. Evidence of oxidative stress following the viral infection of two lepidopteran insect cell lines. Free Radic Biol Med **31:**1448-1455.
81. **Dostert C, Jouanguy E, Irving P, Troxler L, Galiana-Arnoux D, Hetru C, Hoffmann JA, Imler JL.** 2005. The Jak-STAT signaling pathway is required but not sufficient for the antiviral response of *Drosophila*. Nat Immunol **6:**946-953.
82. **Lemaitre B, Hoffmann J.** 2007. The host defense of *Drosophila melanogaster*. Annu Rev Immunol **25:**697-743.
83. **Avadhanula V, Weasner BP, Hardy GG, Kumar JP, Hardy RW.** 2009. A novel system for the launch of alphavirus RNA synthesis reveals a role for the Imd pathway in arthropod antiviral response. PLoS Pathog **5:**e1000582.

967

968 **FIGURE LEGENDS**

969 **Figure 1**

970 *T. ni* and AcMNPV mRNA reads as a percentage of total mRNA reads at each
971 time point from 0 to 72 h p.i.. The percentages of AcMNPV mRNA reads in the
972 infected midgut are indicated by the dashed line (right Y-axis) and the percentage
973 of *T. ni* mRNA reads in the infected midgut are shown as a solid line (left Y-axis).
974 *T. ni* reads were identified by mapping cleaned reads to the *T.ni* genome, and
975 AcMNPV reads were identified by mapping cleaned reads to the AcMNPV
976 genome.

977

978 **Figure 2**

979 Numbers of differentially expressed (DE) *T. ni* transcripts identified in the midgut
980 following AcMNPV infection. Transcriptomes of control (uninfected) and
981 infected *T. ni* midguts were compared and differentially expressed transcripts with
982 at least a 4-fold change and *P*-values <0.05 were identified at each time point (0,
983 6, 12, 18, 24, 36, 48, and 72 h p.i.). Based on the degree of up- or downregulation
984 at each time point, DE transcripts were further classified as induced, upregulated,
985 suppressed, or downregulated transcripts. *T. ni* transcripts with RPKM values of
986 ≤1 in one of the midgut samples (uninfected or infected) were classified as either
987 induced or suppressed transcripts, respectively. If transcript RPKM values were
988 ≥1 in both infected and uninfected midguts (and they differed by ≥4-fold), they
989 were classified as either upregulated or downregulated transcripts.

990

991 **Figure 3**

992 Gene ontology (GO) terms assigned to *T. ni* transcripts that were either
993 upregulated (A), downregulated (B), induced (C), or suppressed (D) in the midgut
994 following AcMNPV infection. Upregulated, downregulated, induced, or
995 suppressed transcripts from all the time points were combined to run Blast2go
996 analysis. GO terms were assigned to the DE transcripts under biological process

with an *E*-value hit filter of 10^{-6} and an annotation cutoff of 55. Also, the GO terms were classified at GO level 4.

Figure 4

Venn diagrams demonstrating numbers of differentially expressed (DE) *T. ni* transcripts that were identified (at each time, and commonly) across the indicated times postinfection, following oral infection with AcMNPV OBs. For Venn diagram construction, we grouped time points into three major classes: Early (0, 6, 12, 18 h p.i.), Middle (24, 36 h p.i.) and Late (48 and 72 h p.i.). Within the early group, time points: 0 and 6 h p.i. contained very few DE *T. ni* transcripts and those transcripts were not common among other time points. Therefore 0 and 6 h p.i. are not shown in the figure. Each circle represents the combined number of differentially expressed genes (induced and upregulated transcripts (A) and suppressed and downregulated transcripts (B)) for the indicated time point (for example-12 h, 18 h, etc.) post infection.

Figure 5

Patterns of differentially expressed (DE) *T. ni* genes following AcMNPV infection of the midgut. A. A cluster analysis of DE *T. ni* midgut transcripts is shown as a heatmap that was generated by performing hierarchical cluster analysis on normalized read counts (log2 transformed) of DE transcripts from infected midgut samples from 0 to 72 h p.i.. Normalized read counts from each biological replicate were averaged, then the averaged normalized read counts of 0 h p.i. were subtracted from each time point's normalized read counts. Euclidean distance metrics were then applied to the normalized read counts using R software. In the illustrated heatmap, the expression levels of each gene (rows) at each time point (columns) are depicted with a color scale in which green represents low level expression and red represents high level expression. The cluster analysis grouped DE transcripts into five clusters based on their expression levels. The groups were arbitrarily assigned the names G1, G2, G3, G4, and G5. B. From the list of *T. ni* transcripts grouped by the cluster analysis, transcripts

with specific patterns (as indicated) were identified using an R script and named P1-P4.

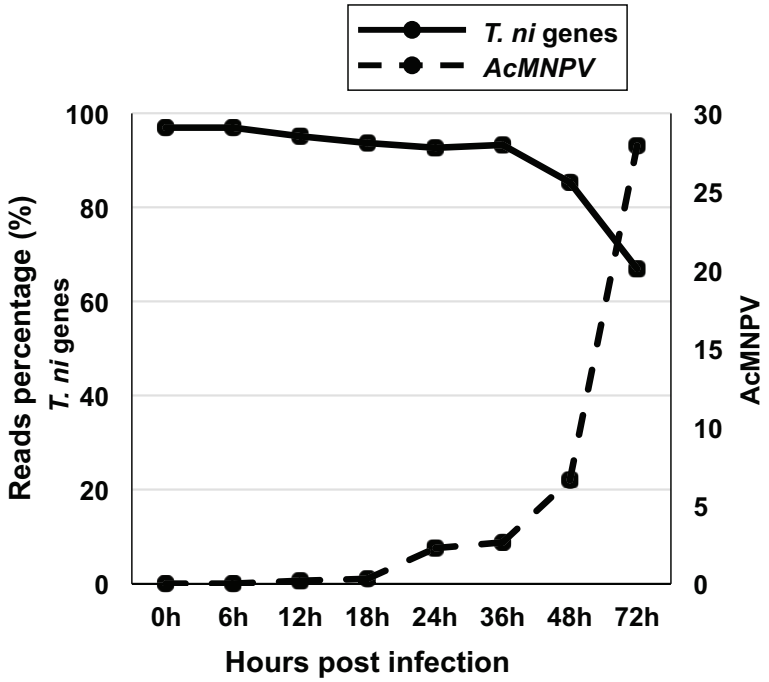
T. ni genes
AcMNPV
Reads percentage (%)
T. ni genes
AcMNPV
100
80
60
40
20
0
30
25
20
15
10
5
0
0h
6h
12h
18h
24h
36h
48h
72h
Hours post infection

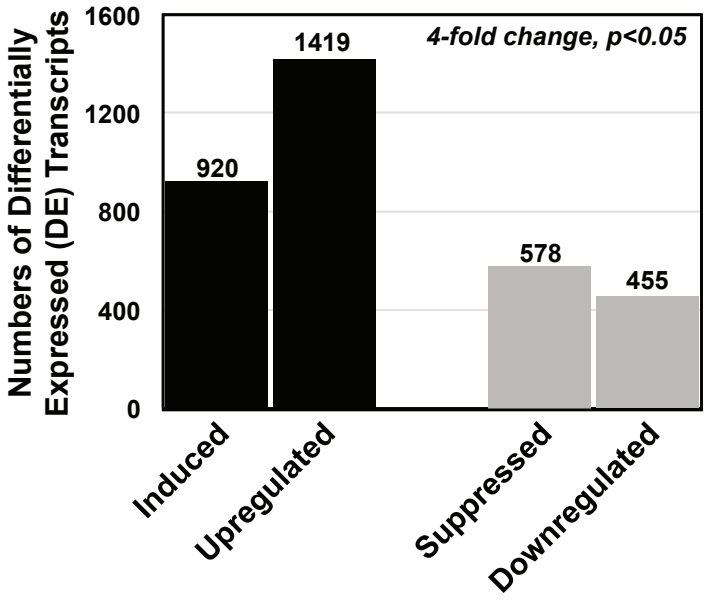
Numbers of Differentially Expressed (DE) Transcripts
1600
1200
800
400
0
4-fold change, p<0.05
920
1419
578
455
Induced
Upregulated
Suppressed
Downregulated

A. Upregulated transcripts

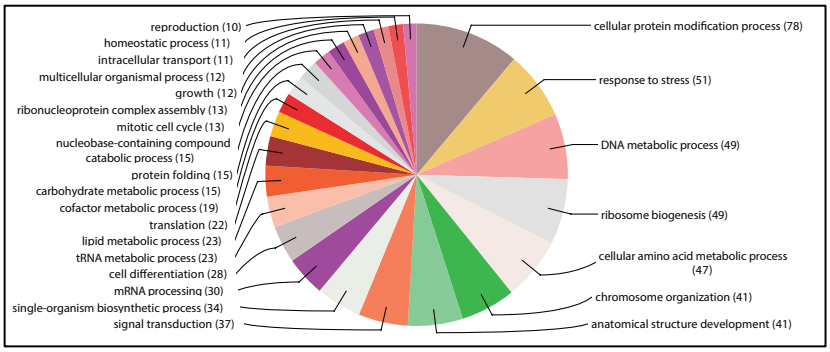

B. Downregulated transcripts

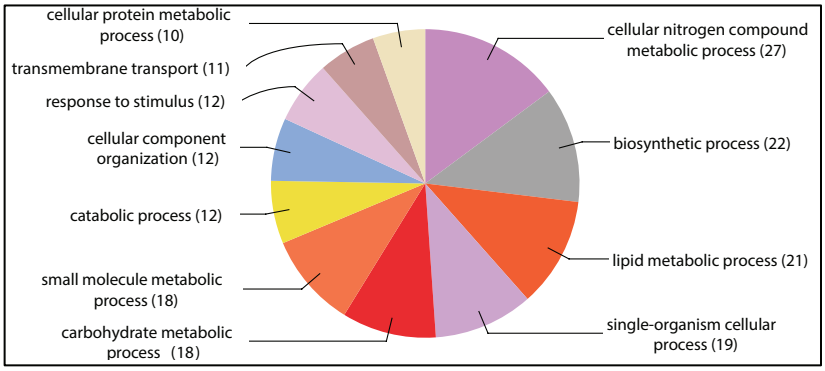

C. Induced transcripts

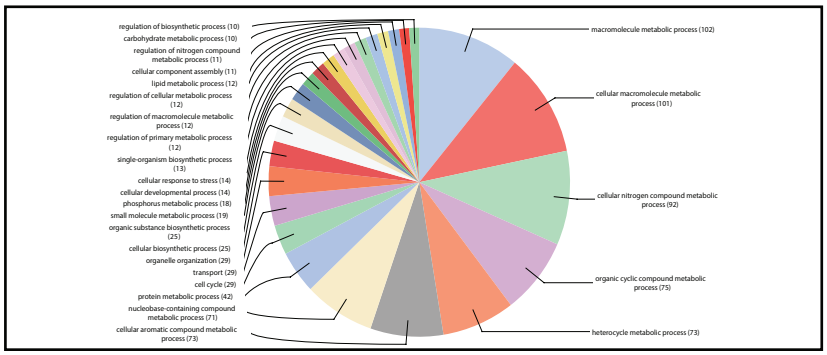

D. Suppressed transcripts

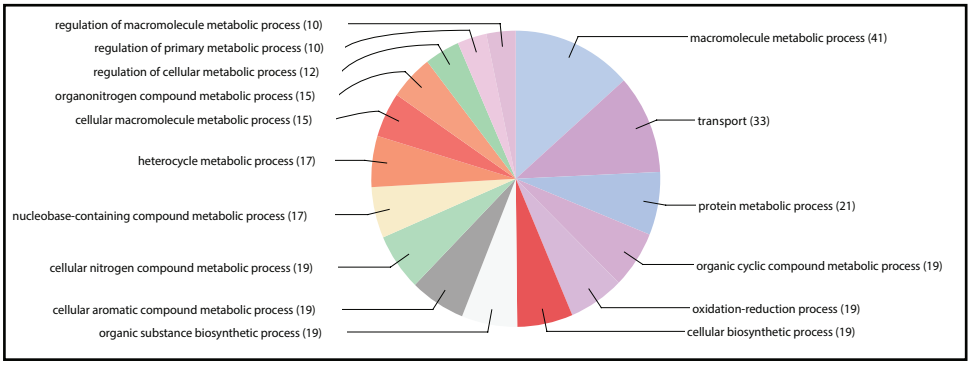

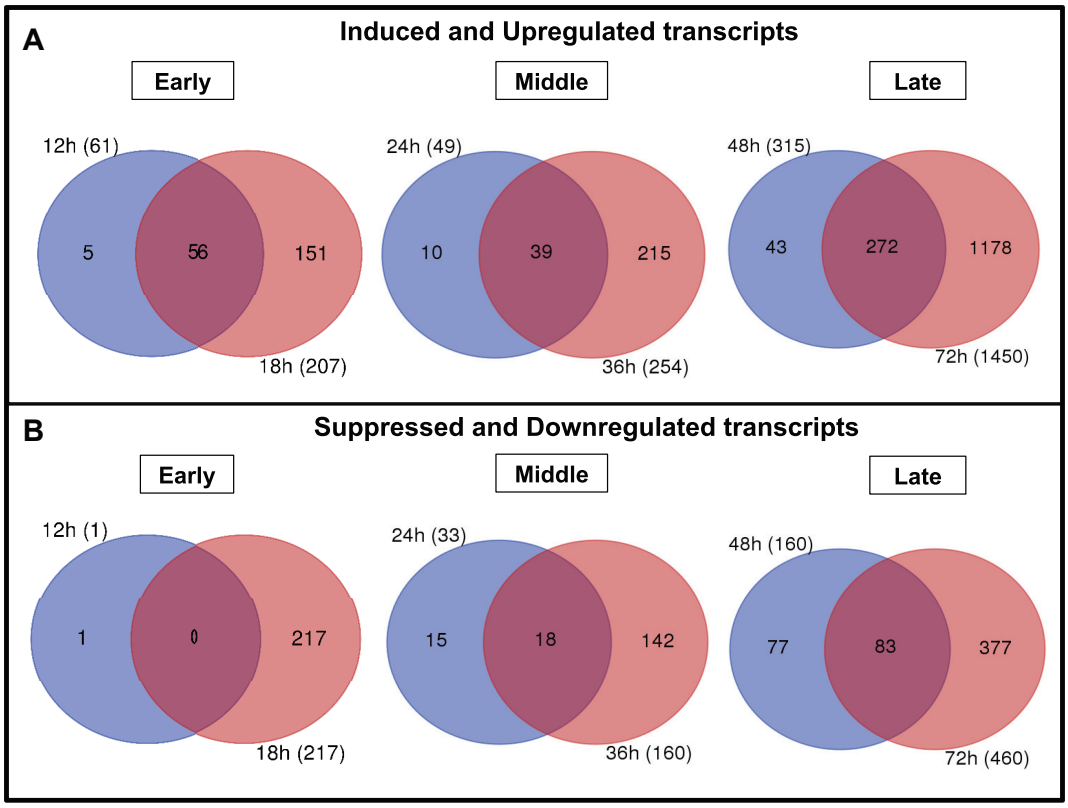
A
Induced and Upregulated transcripts
Early
Middle
Late
12h (61)
5
56
151
18h (207)
24h (49)
10
39
215
36h (254)
48h (315)
43
272
1178
72h (1450)
B
Suppressed and Downregulated transcripts
Early
Middle
Late
12h (1)
1
0
217
18h (217)
24h (33)
15
18
142
36h (160)
48h (160)
77
83
377
72h (460)

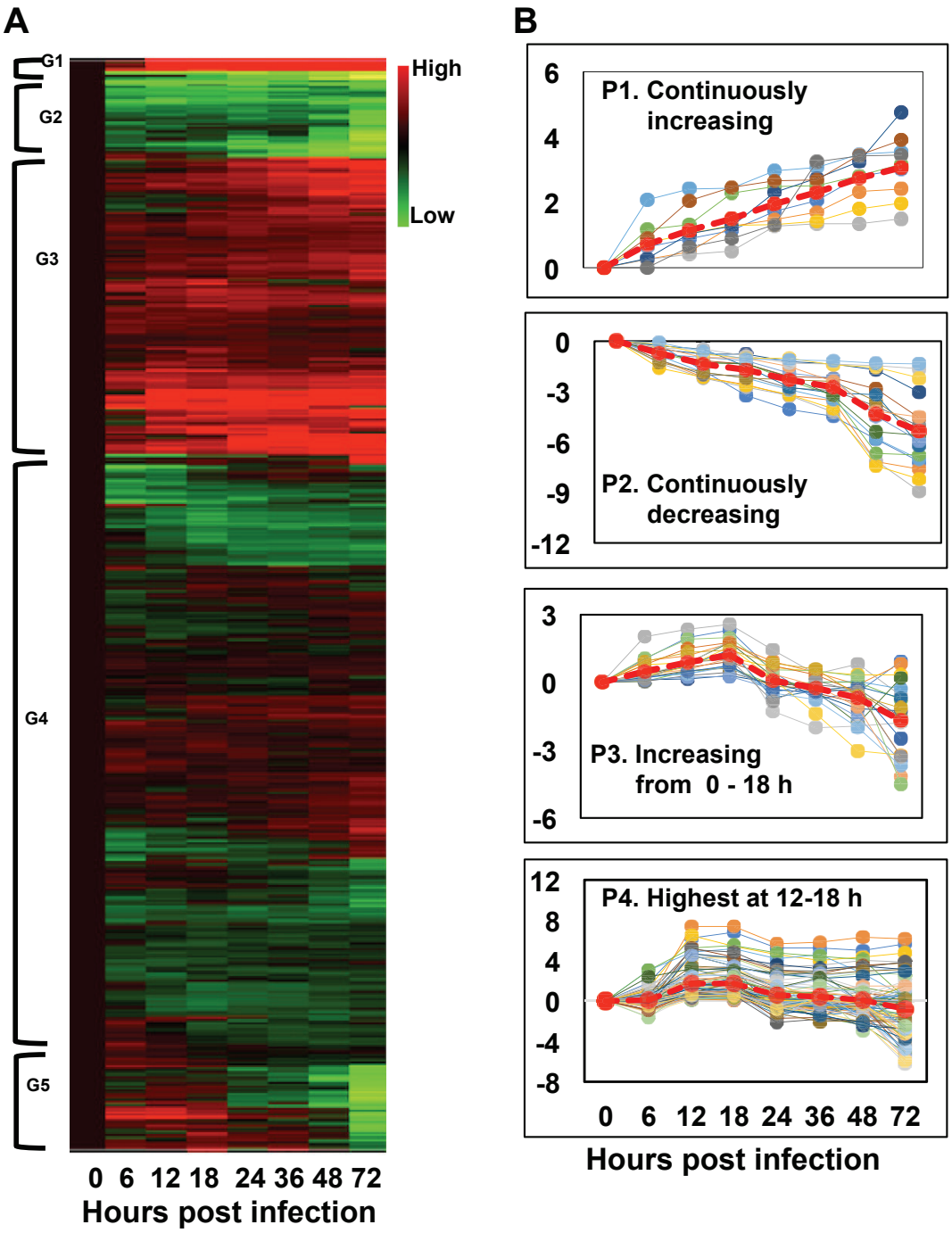
A
G1
G2
G3
G4
G5
High
Low
0 6 12 18 24 36 48 72
Hours post infection
B
6
4
2
0
P1. Continuously increasing
0
-3
-6
-9
-12
P2. Continuously decreasing
3
0
-3
-6
P3. Increasing from 0 - 18 h
12
8
4
0
-4
-8
P4. Highest at 12-18 h
0 6 12 18 24 36 48 72
Hours post infection

Table 1

Reads mapped to *T. ni* and AcMNPV genomes at selected times postinfection

Midgut	Hours post infection	Replicate 1		Replicate 2		Replicate 3		Average midgut reads /time	STDEV of midgut reads/ time
		Total midgut reads*	Total viral reads**	Total midgut reads*	Total viral reads**	Total midgut reads*	Total viral reads **		
Uninfected	0h	18,118,667		21,669,642		21,991,275		20,593,195	2,149,029
	6h	12,283,390		24,758,172		23,153,004		20,064,855	6,786,571
	12h	36,144,710		18,045,491		14,956,667		23,048,956	11,445,929
	18h	14,187,003		17,376,890		14,063,937		15,209,277	1,878,216
	24h	20,763,048		22,762,824		29,499,957		24,341,943	4,577,511
	36h	15,502,539		14,570,698		15,956,828		15,343,355	706,643
	48h	18,503,664		21,009,161		19,745,105		19,752,643	1,252,766
	72h	21,065,355		18,499,850		27,517,673		22,360,959	4,646,421
Infected	0h	17,265,342	338	21,207,395	936	18,567,336	355	19,013,358	2,008,519
	6h	16,151,868	3,447	14,914,261	1,820	17,645,289	2,727	16,237,139	1,367,509
	12h	27,671,909	22,533	13,985,653	62,733	20,895,221	15,008	20,850,928	6,843,236
	18h	19,468,923	68,144	26,218,310	53,738	19,626,036	90,472	21,771,090	3,852,207
	24h	22,069,640	490,621	16,689,213	440,689	14,227,179	301,487	17,662,011	4,010,711
	36h	24,329,106	873,311	13,722,447	436,217	17,663,295	266,238	18,571,616	5,361,351
	48h	14,280,612	388,477	12,411,359	1,341,304	15,288,279	1,247,384	13,993,417	1,459,804
	72h	11,468,070	4,554,198	11,213,699	4,341,483	17,993,483	6,800,054	13,558,417	3,842,985

* Numbers represent Total read counts mapped to the assembled *T. ni* genome (http://www.tnibase.org/cgi-bin/index.cgi) in three biological replicates of *T. ni* midgut samples at each indicated time post infection using HISAT allowing 2 mismatches.

**Numbers represent Total reads mapped to the AcMNPV genome in three replicates of *T. ni* midgut samples using HISAT allowing 2 mismatches. Data from "Infected" rows were reported in Shrestha et al 2018 (J. Virology 92:e01277-01218).

Table 2

T. ni transcripts that are differentially expressed at most times postinfection								
Type of differential expression	***T. ni* gene ID ***	**Annotation**	**Fold change****					
			12 h p.i.	**18 h p.i.**	**24 h p.i.**	**36 h p.i.**	**48 h p.i.**	**72 h p.i.**
Induced and Upregulated	Tni20G02130	HMG176 isoform (REPAT)	IND	IND	IND	IND	IND	79.93
	Tni16G00620	E3 ubiquitin- ligase SIAH1	20.76	IND	5.43	10.37	10.49	15.04
	Tni22G05470	Cyclic GMP-AMP synthase isoform X2	59.07	47.49	5.89	18.06	15.69	35.66
	Tni17G02590	Mitochondrial uncoupling 4	10.77	30.94	14.17	15.86	17.83	47.83
	Tni05G05890	Atlastin-2-like isoform X1	81.19	111.60	9.27	28.72	13.24	49.69
	Tni08G01410	NFX1-type zinc finger-containing 1	IND	IND	8.06	IND	16.47	48.08
	Tni02G00330	NF-kappa-B-repressing factor	5.38	IND	16.33	IND	IND	IND
	Tni14G02910	E3 SUMO- ligase KIAA1586	IND	IND	IND	IND	IND	IND
	Tni16G04790	No blast hits	9.22	IND	4.68	11.00	7.34	16.80
	Tni28G01940	ATP-dependent RNA helicase DHX30	IND	15.16	7.30	IND	9.80	IND
	Tni27G01530	Microphthalmia-associated transcription factor	IND	IND	IND	IND	IND	IND
Suppressed and Downregulated*	Tni18G00450	Serine protease 33	-	SUP	SUP	SUP	SUP	SUP
	Tni17G04440	Folylpolyglutamate synthase	-	-58.97	-66.20	-149.39	-87.98	SUP
	Tni12G01810	Ves G 1 allergen	-	-83.11	-62.53	-92.93	SUP	-97.38
	Tni15G03390	Indole-3-glycerol phosphate synthase	-	SUP	SUP	SUP	SUP	SUP
	Tni21G02480	Flippase	-	-128.95	-290.79	-640.00	-344.40	SUP
	Tni06G03550	DNA mismatch repair protein	-	SUP	SUP	SUP	SUP	SUP
	Tni05G06480	No blast hits	-	-345.04	SUP	SUP	-59.01	-138.96
	Tni15G05500	Hypothetical protein FOXG_02896	-	-60.94	SUP	SUP	-74.40	-36.60
	Tni19G00950	Ionotropic receptor	-	SUP	SUP	SUP	SUP	SUP
	Tni15G06910	Uncharacterized protein LOC110836755	-	SUP	SUP	SUP	SUP	SUP
	Tni15G03460	Unknown	-	-90.55	-46.82	-31.60	-26.10	-15.49
	Tni26G00190	Uncharacterized protein LOC103522958	-	SUP	SUP	SUP	SUP	SUP
	Tni15G04210	Hypothetical protein PABG_01059	-	SUP	SUP	SUP	SUP	SUP
	Tni19G04480	Hypothetical protein X975_10841	-	-14.83	-114.47	-13.32	-95.95	-33.00

For suppressed and downregulated transcripts, commonly expressed transcripts were not identified at 12 h p.i., as indicated by a "-".

**T. ni* gene ID numbers correspond to annotations at: http://www.tnibase.org/cgi-bin/index.cgi

**Fold changes in *T. ni* transcript levels between uninfected and infected midgut samples at selected times postinfection. IND= Induced. SUP=Suppressed.

Table 3

T. ni transcripts significantly affected by AcMNPV infection							
Hours post infection	Type of differential expression	*T. ni* Gene ID*	Annotation	RPKM values		Fold Change	Adjusted p-value
				Control	Infected		
12 h p.i.	Induced	Tni07G03860	C19orf12 homolog	0.56	235.72	IND	-
		Tni20G02130	HMG176 isoform (REPAT)	0.14	97.96	IND	-
	Upregulated	Tni05G05890	Atlastin-2-like isoform X1	7.11	577.24	81.19	4.553E-05
		Tni22G05470	Cyclic GMP-AMP synthase isoform X2	2.55	150.63	59.07	2.033E-22
		Tni17G02340	E3 ubiquitin- ligase SIAH1	3.49	149.59	42.82	1.895E-05
18 h p.i.	Induced	Tni07G03860	C19orf12 homolog	0.50	214.47	IND	-
		Tni12G01690	zinc finger CCHC domain-containing	0.23	188.49	IND	-
	Upregulated	Tni05G05890	Atlastin-2-like isoform X1	7.34	819.13	111.60	1.211E-10
		Tni06G03350	Collagen triple helix repeat domain	47.19	1893.30	40.12	3.392E-02
		Tni08G03170	Cuticle CPH43	34.63	1301.27	37.58	1.547E-05
		Tni16G00140	Immune-related Hdd13	17.37	284.10	16.36	1.649E-02
		Tni03G01880	Mucin-5AC-like	19.11	309.78	16.21	2.117E-03
	Suppressed	Tni15G03390	indole-3-glycerol phosphate synthase	188.57	0.72	SUP	-
		Tni15G03790	EF-hand domain-containing 1	108.99	0.55	SUP	-
	Downregulated	Tni11G00910	Calcium-binding P-	328.38	1.32	-248.77	7.515E-16
		Tni15G03490	E3 ubiquitin- ligase RNF180-like	781.49	7.21	-108.39	3.856E-55
		Tni21G02480	Flippase	1573.23	12.20	-128.95	4.109E-32
		Tni11G03900	Collagen alpha-1(IX) chain isoform X8	201.25	3.41	-59.02	1.317E-31
		Tni17G02150	3-dehydroecdysone 3 alpha-reductase	879.10	21.67	-40.57	6.361E-28
		Tni17G04440	Folylpolyglutamate synthase	433.41	7.35	-58.97	8.603E-12
24 h p.i.	Upregulated	Tni20G02140	HMG176 isoform (REPAT)	1.56	53.16	34.00	1.337E-13
	Downregulated	Tni21G02480	Flippase	747.33	2.57	290.79	8.818E-03
		Tni19G04480	Hypothetical protein X975_10841	606.70	5.30	114.47	3.934E-02
36 h p.i.	Upregulated	Tni08G03170	Cuticle CPH43	27.15	4263.95	157.03	9.743E-17
		Tni03G01880	Mucin-5AC-like	15.72	909.25	57.85	6.327E-05
		Tni20G02110	HMG176 isoform (REPAT)	51.24	833.39	16.26	1.681E-12
	Suppressed	Tni15G05500	hypothetical protein FOXG_02896	109.98	0.98	SUP	-
	Downregulated	Tni21G02480	Flippase	2246.39	3.51	-640.00	2.499E-118
		Tni15G03490	E3 ubiquitin- ligase RNF180-like	596.65	4.99	-119.57	7.924E-50
		Tni17G02150	3-dehydroecdysone 3 alpha-reductase	395.41	10.84	-36.48	2.384E-50
48 h p.i.	Upregulated	Tni07G03860	C19orf12 homolog	3.58	156.25	43.69	2.885E-27
		Tni08G03170	Cuticle CPH43	178.29	3191.83	17.90	1.821E-03
		Tni03G01880	Mucin-5AC-like	59.43	965.99	16.25	3.391E-12
	Suppressed	Tni12G01810	Ves G 1 allergen	105.21	0.86	SUP	-
		Tni11G00910	calcium-binding P-	104.82	0.48	SUP	-
	Downregulated	Tni21G02480	Flippase	1277.72	3.71	-344.40	1.232E-23
		Tni15G03490	E3 ubiquitin- ligase RNF180-like	584.42	7.77	-75.21	1.163E-77
		Tni19G04480	Hypothetical protein X975_10841	544.03	5.67	-95.95	1.155E-04
72 h p.i.	Upregulated	Tni12G01690	Zinc finger CCHC domain-containing	4.65	760.51	163.43	3.673E-24
		Tni05G05890	Atlastin-2-like isoform X1	22.02	1094.12	49.69	2.850E-21
		Tni08G03170	Cuticle CPH43	193.19	7433.26	38.48	8.137E-04
		Tni18G02870	Chymotrypsin-like serine protease	4.04	149.54	37.05	2.575E-10
		Tni22G05470	Cyclic GMP-AMP synthase isoform X2	4.67	166.64	35.66	1.161E-17
		Tni26G01100	Zinc finger	10.28	297.86	28.98	3.497E-17
		Tni03G01880	Mucin-5AC-like	76.58	1523.70	19.90	1.234E-04
		Tni22G00330	Peroxidase isoform X2	16.99	273.16	16.07	1.895E-04
	Suppressed	Tni11G00910	calcium-binding P-	287.35	0.66	SUP	-
		Tni19G04800	ninjurin-2 isoform X1	236.30	0.85	SUP	-
		Tni08G02780	Carboxypeptidase M	156.34	0.78	SUP	-
		Tni18G00450	serine protease 33	148.55	0.33	SUP	-
		Tni23G01020	surface protective antigen	87.18	0.08	SUP	-
	Downregulated	Tni08G00710	Peritrophic matrix insect intestinal	305.78	1.10	-277.98	1.379E-04
		Tni04G00650	Stress response NST1 isoform X1	420.33	1.88	-223.58	1.915E-56
		Tni13G03290	Abhydrolase domain-containing 7	721.86	9.99	-72.26	7.879E-44
		Tni12G01650	Calponin transgelin	812.78	8.97	-90.61	7.243E-42
		Tni15G03490	E3 ubiquitin- ligase RNF180-like	684.19	8.30	-82.43	1.339E-02
		Tni11G02810	Lipase 3	473.89	8.30	-57.10	6.491E-10
		Tni15G01350	Zinc metalloproteinase nas-4-like	355.98	6.69	-53.21	6.499E-07
		Tni22G01200	27 kDa hemolymph	634.65	21.15	-30.01	4.057E-35
		Tni03G02090	Moderately methionine rich storage	642.02	20.51	-31.30	7.960E-23
		Tni17G05550	Cytochrome P450	237.62	7.40	-32.11	2.547E-16
		Tni18G04160	Ecdysone oxidase	273.31	12.45	-21.95	2.347E-20
		Tni13G00880	Cobatoxin short form A	572.15	26.23	-21.81	1.092E-10

*_T. ni_ gene ID numbers correspond to annotations at: http://www.tnibase.org/cgi-bin/index.cgi

Significantly affected _T. ni_ transcripts consist of at least 16 fold change in expression levels and 50 RPKM values in control (uninfected) or infected midgut samples. IND= Induced. SUP=Suppressed.